DOI: 10.1002/zaac.200900051

Crystal Structure Refinement and Electronic Properties of Si(*cI*16)

Aron Wosylus,[a] Helge Rosner,[a] Walter Schnelle,[a] and Ulrich Schwarz*[a]

Dedicated to Prof. Reinhard Nesper on the Occasion of His 60th Birthday

Keywords: Silicon; Allotropy; Crystal structure; Electronic density of states; Physical properties

Abstract. Si(*cI*16) is prepared in polycrystalline form at 12(1.5) GPa at temperatures between 800(80) K and 1200(120) K. The crystal structure is refined by a full-profile method using x-ray powder diffraction data. Si(*cI*16) is diamagnetic ($\chi_0 = -5.6(1.8) \times 10^{-6}$ emu·mol^{-1}) and shows a weakly temperature-dependent electrical resistivity [$\rho(300\ \mathrm{K}) = 0.3 \times 10^{-3}\ \Omega\cdot\mathrm{m}$]. Computations of structural and electronic properties of Si(*cI*16) within the local density approximation evidence the metastable character of the allotrope with respect to diamond-type silicon. The calculations yield a positional parameter which is in perfect agreement with the refined value. In agreement with the experimentally observed electrical conductivity properties, the computed density of states evidence that the Fermi level of Si(*cI*16) is located in a pseudo-gap.

Introduction

In the course of investigations on binary tetrelides of alkaline-earth metals manufactured at high-pressure high-temperature conditions [1−4], we observed the metastable element modifications Ge(*tP*12) [5, 6] and Si(*cI*16) [7] as minority phases after application of pressures slightly above ten GPa with a large-volume two-stage multi-anvil device. Si(*cI*16) was described for the first time more than forty years ago. The crystal structure (Figure 1) was solved on the basis of x-ray powder diffraction data, but the position parameter of silicon was only estimated by visual comparison of experimental and calculated x-ray diffraction intensities. In the atomic arrangement which is isotypic to Ge(*cI*16) [8], tetracoordinated silicon atoms are reported to adopt a trigonal pyramidal coordination with *d*(Si−Si) of $1 \times 2.369(9)$ Å and $3 \times 2.384(9)$ Å [7] instead of tetrahedral with *d*(Si−Si) = 2.351 Å [9] in ambient pressure Si(*cF*8).

Later in-situ investigations at high pressures [10] including studies of the formation of Si(*cI*16) at elevated temperatures [11] as well as determinations of the electrical resistance were performed on minute samples using the diamond anvil cell technique [12]. The results evidence that, at ambient temperature, the phase Si(*cI*16) is metastable between ambient pressure and at least 2 GPa. Transformation at normal pressure requires heating to 423 K for several hours [7].

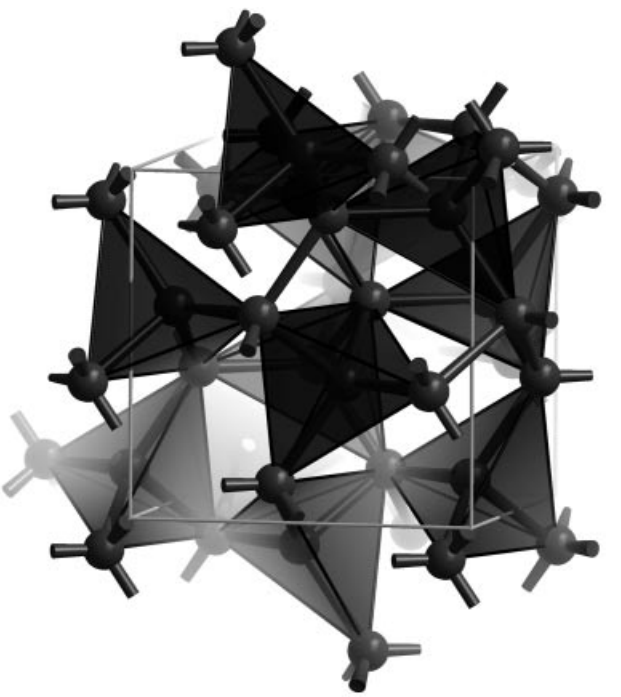

Figure 1. Crystal structure of Si(*cI*16). Short interatomic distances *d*(Si−Si) = 2.35 ± 0.04 Å which are compatible with covalent single bonds are emphasized by dark lines. Distorted trigonal pyramidal coordination polyhedra are shaded. The cubic unit cell is indicated by thin grey lines.

The renewed interest in crystal structure and physical properties of Si(*cI*16) is motivated by the lack of refined structural data and magnetic measurements as well as by the importance of the allotrope as a prototype tetrahedral framework with a differentiation of interatomic distances due to a decrease of symmetry. We report herein the least-

* PD Dr. U. Schwarz
Fax: +49-351-4646-4002
E-Mail: schwarz@cpfs.mpg.de
[a] Max-Planck-Institut für Chemische Physik fester Stoffe
Nöthnitzer Straße 40
01187 Dresden, Germany

squares refinement of crystal structure parameters using x-ray powder diffraction data and measurements of magnetic properties and electrical resistivity. Concomitant band structure calculations independently evaluate the stability of the allotrope and the refined structural parameter. Moreover, they shed light on the electronic structure and the specific changes caused by the deviation of the coordination polyhedron from tetrahedral symmetry.

Experiments and Band Structure Calculations

Si(*cI*16) was synthesized from the starting material Si(*cF*8) (Alpha Aesar 99.9999 %) at 12(1.5) GPa and temperatures between 800(100) K and 1200(120) K in a hydraulic press equipped with a Walker-type module [13, 14]. Typically, pressure was increased within 4 h and released within 10 h. Pressure calibration had been performed prior to the experiments measuring the resistance changes associated with the phase transitions of bismuth [15] and lead [16−18]. The temperature-current relation had been determined in separate runs with W/WRe thermocouples. Heating was realized with graphite tubes. Hexagonal boron nitride served as crucible material. No apparent reaction with silicon at the selected transformation conditions was observed. X-ray powder diffraction experiments were performed in transmission arrangements (Huber Image Plate G670 with Cu-$K_{\alpha 1}$ radiation and at ID31 of the ESRF using a high-resolution set-up and synchrotron radiation). Details concerning measurement and refinement as well as selected results are given in Table 1.

Table 1. Details of the diffraction measurements and crystallographic data of Si(*cI*16). Refinements are carried out with the computer program WinCSD [27]. Rietveld refinements are performed using Fullprof [28]. A Pseudo-Voigt function is used for profile simulation and a sixth order polynomial for modelling the background.

Compound	Si(*cI*16)
Space group (No.)	$Ia\bar{3}$ (206)
Lattice parameters: Rietveld refinement of synchrotron data; Laboratory source with LaB_6 standard	6.6265(1) Å; 6.6229(2) Å
Earlier data	6.64(1) [7]
Unit cell volume /Å^3	290.97(1)
Refined position parameter Si(*x, x, x*)*	0.10143(4);
Earlier data	0.103(1) [7]; 0.1025 [10]
$U_{11} = U_{22} = U_{33} = U_{eq}$ /Å^2	0.0058(2),
$U_{12} = U_{13} = U_{23}$ /Å^2	0.0003(2)
Z	16
Calculated density /g·cm^{-3}	2.564;
Earlier data	2.55 [7]
Diffractometer, wave length λ /Å	ESRF ID31, 0.39987(2)
Diffraction set-up; Quartz capillary	Transmission alignment; d = 1 mm
Number of reflections;	97
$2\theta_{max}$ /degree, step width /degree	36, 0.005
Residuals R_p; R_{wp}; R_{exp}	5.82; 7.84; 1.65
Interatomic distances with experimental errors as calculated in the full profile refinements*	1 × 2.3283(4) Å; 3 × 2.3841(4) Å; 1 × 3.4104(4) Å
Earlier data	2.369(9) Å [7]; 2.384(9) Å [7]; 3.381(9) Å [7]
Angles / Degree	98.70(1); 117.75(1)
Earlier data	98.1(3) [7]; 118.0(4) [7]

* The maximal error of the internal coordinate as estimated on the basis of the number of observed reflections corresponds to 0.002.

The samples for the physical measurements on Si(*cI*16) were two polycrystalline pieces from separate high-pressure synthesis runs. The magnetization was determined in magnetic fields $\mu_0 H$ = 3.5 T and 7 T between 1.8 K and 300 K and also at lower fields in a SQUID magnetometer (MPMS XL-7, Quantum Design). The sample consisted of two pieces with a total mass of 27.82 mg co-mounted with GE-7031 varnish to a thin quartz rod. Corrections for the sample holder and the glue were applied. The electrical resistance was measured with a linear four-point method using alternating current in the temperature range 1.8−380 K. For that purpose one piece was ground to dimensions 1.85 × 1.90 × 1.14 mm. Due to the uncertainties of the contact distance and the cross-section the estimated inaccuracy of the electrical resistivity is ±30 %. For comparison the resistivity data of another piece (dc measurement, 4−320 K) are given.

For electronic structure calculations the full-potential local-orbital scheme FPLO (version: FPLO 8.00−31) within the local density approximation (LDA) was used [19]. In the scalar relativistic calculations the exchange and correlation potential of Perdew and Wang was chosen [20]. To ensure accurate total energy and density of states (DOS) information, a fine, well converged *k*-mesh of 9486 points in the irreducible part of the Brillouin zone was used.

Results and Discussion

Within the investigated pressure and temperature range, syntheses yield polycrystalline single-phase Si(*cI*16) in all experiments. X-ray powder diffraction patterns (Figure 2) reveal a significant peak broadening, e.g., for the strongest reflection (121) a full width at half maximum of 0.08° at 2θ = 8.477°. By applying the *Scherrer*-equation [21], this corresponds to an average domain size of roughly 250 Å. The small particle dimension is attributed to a first-order transition of the intermediate high-pressure phase Si(*hR*8) into Si(*cI*16) at pressures around 2 GPa [10] upon decompression.

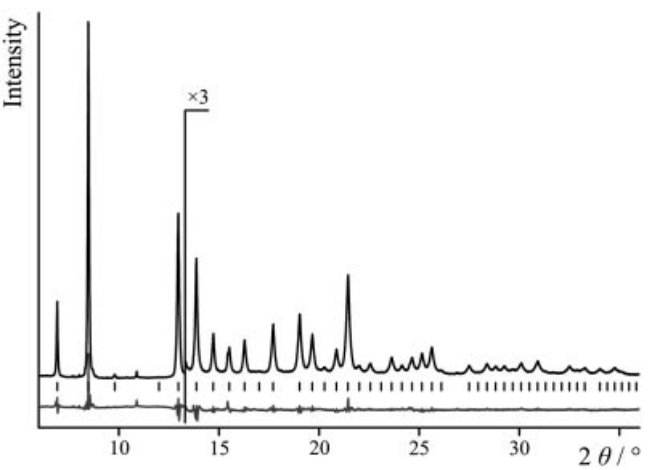

Figure 2. X-ray powder diffraction diagram of Si(*cI*16) recorded using low-divergence synchrotron radiation at ID31 of the ESRF (λ = 0.39987(2) Å). The grey curve corresponds to the difference between observed and calculated intensities multiplied by a factor of three. Reflection positions are indicated by vertical bars.

The structure model of the earlier solution is refined by means of a least-squares procedure using complete x-ray powder diffraction diagrams (Figure 2). The supposed atomic arrangement [7] is essentially confirmed by the results with the main exception that the present analysis of the high-quality synchrotron x-ray diffraction intensities evidences a difference of the crystallographically independent interatomic distances of about 0.06 Å (see Table 1). Thus, Si(*cI*16) belongs indeed to the small, but still growing set of high-pressure phases in which the reduction of point symmetry is associated with a differentiation of chemically equivalent interatomic distances [22].

The high-field magnetic susceptibility $\chi(T) = M/H$ (Figure 3, top) of the sample is slightly dependent on field, which indicates minor ferromagnetic impurities. The latter are taken into account with the Honda-Owen extrapolation for each temperature. The weakly temperature-dependent correction applied to the 7 T data corresponds to approximately -1.5×10^{-6} emu·mol^{-1}, which would be consistent with, e.g., a mass fraction of elemental iron of 16×10^{-6}. The resulting susceptibility displays a weak Curie contribution. The intrinsic, essentially temperature-independent susceptibility of Si (*cI*16) is obtained by a fit: $\chi_0(T = 0\ \mathrm{K}) = -5.6(1.8) \times 10^{-6}$ emu·mol^{-1}, the value of $\chi(300\ \mathrm{K})$ is $-5.3(1.5) \times 10^{-6}$ emu·mol^{-1}. For comparison, the value of $\chi(300\ \mathrm{K})$ for Si(*cF*8) is -3.12×10^{-6} emu·mol^{-1} [23] or, according to a different source, -5.3×10^{-6} emu·mol^{-1} [24]. No phase transitions are observed in the covered temperature range.

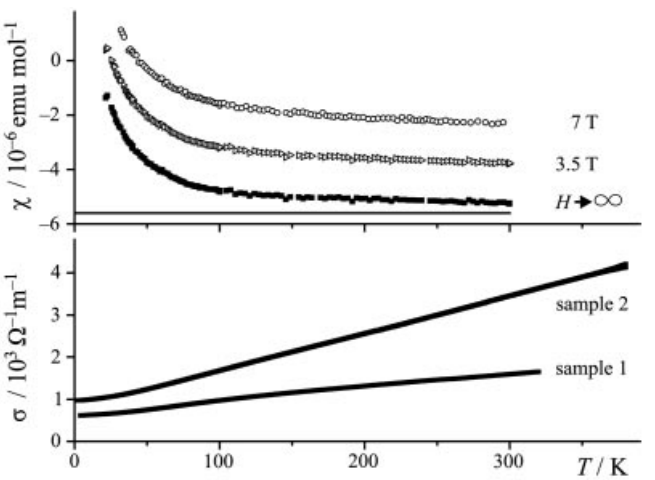

Figure 3. Top: Measured ($\mu_0 H$ = 7.0 T and 3.5 T) and extrapolated ($\mu_0 H \rightarrow \infty$) molar magnetic susceptibility $\chi(T,H)$ of the Si(*cI*16) sample. The grey line indicates the intrinsic temperature-independent term χ_0 for T = 0 K. Bottom: Electrical conductivity $\sigma(T)$ (inverse electrical resistivity) of two Si(*cI*16) samples. The linear dependence above approximately 50 K is consistent with a heavily doped semiconductor.

The temperature dependence of the electrical resistivity is rather weak: from a room-temperature value $\rho(300\ \mathrm{K}) = 0.3 \times 10^{-3}\ \Omega\cdot\mathrm{m}$ the resistivity increases only to $\rho_0 = 1.0 \times 10^{-3}\ \Omega\cdot\mathrm{m}$ at 1.8 K. The value at 100 K of $0.6 \times 10^{-3}\ \Omega\cdot\mathrm{m}$ compares very well with that in a previous investigation [ρ (100 K) = $0.5 \times 10^{-3}\ \Omega\cdot\mathrm{m}$] [12]. In order to check the variation among different samples and primings, we measured a second piece from another synthesis run (see Figure 3b bottom). The conductivity is slightly lower but shows almost the same temperature dependence. For $T > 50$ K and at least up to 350 K the conductivity $\sigma(T)$ of our Si(*cI*16) samples increases linearly with temperature. The same observation for $\sigma(T)$ has been previously attributed to localization effects in a disordered system [12]. Below 10 K, the equation $\sigma(T) = \sigma_0 + aT^{\alpha}$ with $\alpha = 3/2$ can be well fitted to the recent conductivity measurements while in an analysis of earlier data a power law with $\alpha = 2$ has been applied [12].

As an independent approach to both the electronic and the structural features of metastable Si(*cI*16), we applied a highly accurate full-potential band structure scheme to calculate electronic structure and total energies for Si(*cI*16). As a reference, well-known diamond-type Si(*cF*8) is selected. For the experimentally determined lattice parameters at ambient conditions, diamond-type silicon is more stable than the metastable cubic allotrope by an energy difference of about 130 meV per atom (12.6 kJ/mol). For the same unit cell volume, the positional parameter x for Si(*cI*16) was optimized (Figure 4). The equilibrium position is calculated to $x_{\mathrm{theo}} = 0.10149(5)$ in excellent agreement with the experimental value $x_{\mathrm{exp}} = 0.10143(4)$ (see Table 1 and comment therein).

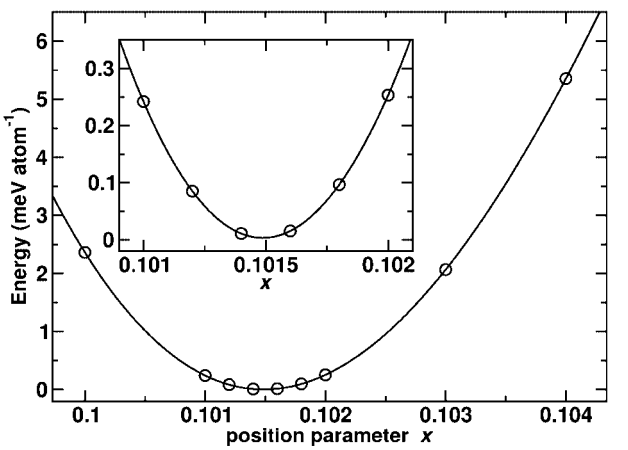

Figure 4. Total energy as a function of the silicon coordinate. Open circles indicate calculated values, black lines represent a least squares fit of a fourth-order polynomial to the data. The minimum of the fitted curve corresponds to $x = 0.10149(5)$ in perfect agreement with the experimental result. The insert shows an enlargement of the curve in the vicinity of the energy minimum.

Figure 5 shows a comparison of the calculated electronic DOS of Si(*cI*16) and Si(*cF*8). We find semiconducting behaviour for the diamond-type phase of silicon with a DOS gap of about 0.5 eV. The underestimation with respect to the experimental value of about 1.1 eV is related to the well-known gap problem of the LDA. In contrast, for Si(*cI*16) we find that the Fermi level ε_F is located in a pronounced pseudo-gap with a low density of states. A corresponding

Zeitschrift für anorganische und allgemeine Chemie ZAAC Journal of Inorganic and General Chemistry

calculation for a model with equidistant neighbours provides rather large values for the DOS at ε_F. Thus, the emergence of the local DOS minimum for Si(*cI*16) is clearly caused by the differentation of the distances *d*(Si−Si) within the trigonal pyramidal coordination.

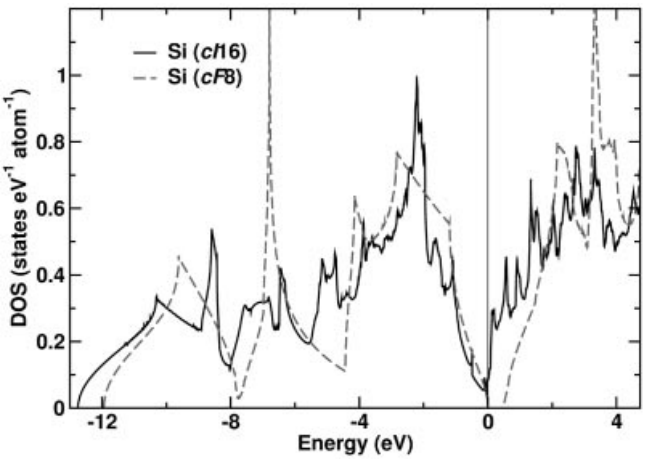

Figure 5. Electronic density of states of Si(*cF*8) and Si(*cI*16). The LDA calculations reveal semiconducting behaviour for diamond-type silicon and a pseudo-gap with a low density of states for the metastable phase.

The valence band width of Si(*cI*16) is slightly larger (about 1 eV) than that of Si(*cF*8). A model with four equivalent distances *d*(Si−Si) and an additional adjustment of the interatomic distances to the value of diamond-type silicon yields a valence band width which is very close to that of Si(*cF*8). This finding reveals that the slightly larger valence band width of Si(*cI*16) compared to diamond-type silicon is mainly caused by the shorter next-neighbour distance.

As a summary, we have collected additional theoretical and experimental evidence for the difference of the symmetry-independent interatomic distances in the trigonal pyramidal coordination sphere of silicon atoms in Si(*cI*16). In accordance with the findings of resistivity measurements, band structure calculations reveal substantial differences of the electronic features which can be traced back to the dissimilarity of the atomic arrangements of Si(*cF*8) and Si(*cI*16). The results concerning total energy and atomic position establish elaborate band structure calculations once more as a valuable and reliable tool for gaining deeper insight into crystal structure properties and phase diagrams of elements [25, 26].

Acknowledgement

For supporting high-pressure synthesis we thank *Carola J. Müller*, *Susann Leipe* and *Knut Range*. Help with the high-resolution X-ray powder diffraction measurements by *Irene Margiolaki*, *Yuri Prots* and *Andreas Schlechte* at the ESRF is gratefully acknowledged. Special thanks to *Ralf Koban* for fastidious sample priming.

References

[1] A. Wosylus, Yu. Prots, U. Burkhardt, W. Schnelle, U. Schwarz, Yu. Grin, *Solid State Sci.* **2006**, *8*, 773.
[2] A. Wosylus, Yu. Prots, U. Burkhardt, W. Schnelle, U. Schwarz, Yu. Grin, *Z. Naturforsch. Teil B* **2006**, *61*, 1485.
[3] A. Wosylus, Yu. Prots, U. Burkhardt, W. Schnelle, U. Schwarz, *Sci. Technol. Adv. Mater.* **2007**, *8*, 383.
[4] A. Wosylus, PhD Thesis, University of Dresden, submitted.
[5] F. P. Bundy, J. S. Kasper, *Science* **1963**, *139*, 340.
[6] A. Wosylus, Yu. Prots, W. Schnelle, U. Schwarz, *Z. Naturforsch. Teil B* **2008**, *63*, 608.
[7] R. H. Wentorf Jr, J. S. Kasper, *Science* **1963**, *139*, 338.
[8] R. J. Nelmes, M. I. McMahon, N. G. Wright, D. R. Allan, J. S. Loveday, *Phys. Rev. B* **1993**, *48*, 9883.
[9] R. R. Reeber, B. A. Kulp, *Transition Met. Soc. AIME.* **1965**, *233*, 698.
[10] J. Crain, G. J. Ackerland, J. R. Maclean, R. O. Piltz, P. D. Hatton, G. S. Pawley, *Phys. Rev. B* **1994**, *50*, 13043.
[11] G. Weill, J. L. Mansot, G. Sagon, C. Carlone, J. M. Besson, *Semicond. Sci. Technol.* **1989**, *4*, 280.
[12] J. M. Besson, E. H. Mokhtari, J. Gonzalez, G. Weill, *Phys. Rev. Lett.* **1987**, *59*, 473.
[13] D. Walker, M. A. Carpenter, C. M. Hitch, *Am. Mineral.* **1990**, *75*, 1020.
[14] H. Huppertz, *Z. Kristallogr.* **2004**, *219*, 330.
[15] I. C. Getting, *Metrologia.* **1998**, *35*, 119.
[16] T. Takahashi, H. Kwang, W. A. Bassett, *Science* **1969**, *165*, 1352.
[17] L. F. Vereshchagin, A. A. Semerchan, N. N. Kuzin, Y. A. Sadkov, *Sov. Phys. Dokl.* **1970**, *15*, 295.
[18] H. Mii, I. Fujishiro, M. Senoo, K. Okawa, *High Temp.-High Pressures* **1973**, *5*, 155.
[19] K. Koepernik, H. Eschrig, *Phys. Rev. B* **1999**, *59*, 1743.
[20] J. P. Perdew, Y. Wang, *Phys. Rev. B* **1992**, *45*, 13244.
[21] P. Scherrer, *Nachr. Ges. Wiss. Göttingen* **1918**, 100.
[22] R. Demchyna, S. Leoni, H. Rosner, U. Schwarz, *Z. Kristallogr.* **2006**, *221*, 420.
[23] *CRC Handbook of Chemistry and Physics*, 87th ed., D. R. Lide (Ed.), CRC Press, Boca-Raton, **2007**.
[24] P. W. Selwood, *Magnetochemistry*, 2nd ed., Interscience, New York, **1956**.
[25] U. Schwarz, L. Akselrud, H. Rosner, A. Ormeci, Yu. Grin, M. Hanfland, *Phys. Rev. B* **2003**, *67*, 214101.
[26] A. Ormeci, K. Koepernik, H. Rosner, *Phys. Rev. B* **2006**, *74*, 104119.
[27] L. G. Akselrud, P. Yu. Zavalii, Yu. Grin, V. K. Pecharski, B. Baumgartner, E. Wölfel, *Mater. Sci. Forum* **1993**, 133.
[28] J. Rodriguez-Carvajal, *Phys. B* **1993**, *192*, 55.

Received: January 19, 2009
Published Online: March 19, 2009

